Eur. Phys. J. D (2019) 73: 71
https://doi.org/10.1140/epjd/e2019-90281-3

THE EUROPEAN PHYSICAL JOURNAL D

Regular Article

Surface and thermal characteristics relationship of atmospheric pressure plasma treated natural luffa fibers

Essam Abdel-Fattah[1,2,a]

[1] Plasma Technology and Material Science Unit (PTMSU), College of Science and Humanities, Prince Sattam Bin Abdulaziz University, PO 173, 11942 Al-Kharj, Saudi Arabia
[2] Physics Department, Faculty of Science, Zagazig University, 44519 Zagazig, Egypt

Received 11 June 2018 / Received in final form 24 September 2018
Published online 2 April 2019

Abstract. In this work, the effects of Ar and He atmospheric pressure plasma on the natural luffa fibers surface and thermal properties were investigated. Optical emission spectroscopy OES has been used to characterize the Ar and He plasmas. The pristine and plasma-treated luffa fibers were analyzed by means of scanning electron microscopy (SEM), Fourier transform infrared spectroscopy (FTIR), X-ray photoelectron spectroscopy (XPS), thermogravimetric analysis (TGA) and water contact angle. The SEM images show the removal of hemicellulose and lignin layers from plasma treated luffa surface, whilst preserve their integrity. This was confirmed by FTIR and XPS results. XPS analysis of the plasma treated luffa fibers revealed the formation of oxygen containing functional groups and hence the O/C ratios increases from 0.18 in pristine to 1.08 and 1.09 in He and Ar plasma treated ones, respectively. This results lead to improvement of the adhesion and wettability characteristics of luffa fiber as well as their thermal stability.

Recently, natural fibers have attracted much interest as eco-friendly products with a potential applications in emerging technologies. Among natural fibers, luffa cylinderica is identified as a potential candidate with a wide range of applications such as cell immobilization for biotechnology [1], supercapacitors [2], packaging [3], water absorption [4,5], and waste water treatment [6]. Luffa fibers exhibit remarkable stiffness and energy absorption capacity [7], elasticity module (3.4 GPa), and specific strength (29.4 MPa) [3,8]. Such good mechanical characteristics make luffa fibers one of the most promising candidates as an eco-friendly reinforce cement fiber in composite industry when compared with traditional fibers such as glass fibers [9,10].

Luffa cylinderica is multidirectional array of fibers composed of cellulose 55–90%, hemicelluloses 8–22%, lignin 10–23%, and extractives-ash 3.6% [8]. In fact, the luffa fiber is considered a miniature composites in which the cellulose framework of the luffa is embedded in a "matrix" of lignin. The lignin by its nature, a kind of wax, weakens the interfacial adhesion properties of the luffa fibers as well as their absorption capacity. Thus, to improve luffa fibers compatibility with the matrix material, it is important to etch, or remove, the lignin outer surface and/or functionalize inner callous frameworks of luffa fibers to enhance their surface reactivity. Various surface treatment technique have been reported to modify luffa fiber surface including mercerization, or alkali treatment [11], hornification, or several cycles of drying and rewetting [12], and ultraviolet radiation graft [13]. Though these methods improve the surface roughness and hence yield better mechanical interlocking. The increasing environmental awareness and time constrains has prompted searching for new eco-friendly technology to improve surface characteristics of luffa fibers. Thus, one of the aims of this work is to study the effect of atmospheric pressure plasma on the surface characteristics of luffa fiber. The advantages of using plasma is not limited to being free from residual chemical contamination, but it also can introduce a wide range of functional groups on the fibers surface in a short span of time. In addition, the plasma species interaction with luffa surface is limited to several angstrom and hence relatively nondestructive, meaning preserve the good bulk properties. When a luffa fiber is exposed to plasma, it is expected that the plasma active species effectively interact with fiber surface inducing modification of the fiber surface characteristics. It is important to understand correlation between the atmospheric pressure plasma parameters and the luffa fibers surface characteristics.

In the current work, luffa fibers are treated by helium and argon atmospheric pressure plasmas. The surface characterization of pristine and plasma treated luffa fibers were characterized by scanning electron microscopy

[a] e-mail: essam29@hotmail.com

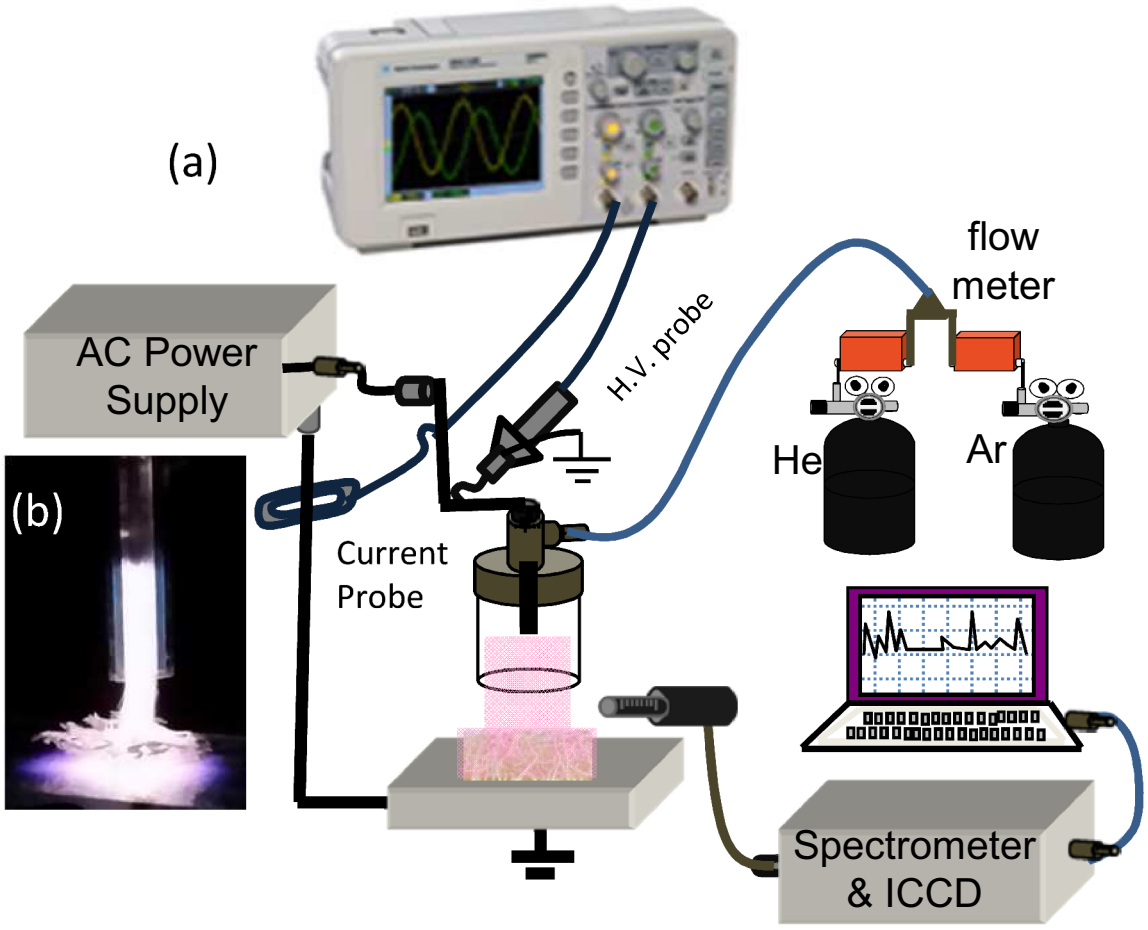

Fig. 1. (a) Schematic diagram of the experimental setup for the atmospheric pressure plasma treatment system, and (b) photo of the APPJ.

(SEM), X-ray photoelectron emission spectroscopy (XPS) and Fourier transform infrared spectroscopy (FTIR). Further more, thermogravimetric analysis (TGA) of the pristine and plasma treated luffa fibers are presented.

1 Experimental setup

Figure 1a shows the atmospheric pressure plasma treatment system with optical emission spectrometer. The atmospheric pressure plasma jet (APPJ) is driven by 17.59 kHz AC voltage. The high-voltage signal is applied to tungsten wire (diameter = 1 mm), that acts as the power electrode. The tungsten wire is placed at the center of a quartz capillary tube with a radius of 3 mm. A grounded aluminum plate is positioned downstream of the quartz tube 20 mm from the high-voltage electrode and 10 mm away from the edge of the capillary tube. The luffa sample is placed on the ground electrode at a fixed distance of 5 mm away from the plasma jet orifice. The discharge is generated inside the quartz tube and diffuses outward, thus plasma treatment is performed in the after glow zone. The gas flow rate is controlled by a gas flow controller with a maximum flow limit of 10 standard liters per minute (slm) for argon and helium gases. The high voltage waveform at the powered electrode was measured using a calibrated 1000:1 high-voltage probe (Tektronix P6015A), directly connected to the powered electrode, meanwhile the discharge current was monitored using a wide band current probe (Pearson 6585). Further, a four-channel DQ8000 digital oscilloscope was employed to display the voltage and current waveforms.

The plasma emission spectra was measured using a Ocean Optics USB2000 spectrometer equipped with a intensified CCD (ICCD) detector, with a spectral range of 240−900 nm. The luffa fibers samples were exposed to Ar or He plasmas for fixed exposure time of 40 s at discharge voltage of 10 kV_{pp} and constant gas flow rate of 3 l min^{-1} for argon and helium gas, respectively. The chemical composition of the pristine and plasma treated luffa surfaces were measured by X-ray photoelectron spectroscopy, using a flood gun for charge compensation. The XPS spectra and data analysis including peak fitting were performed by Thermo Avantage software (version 5.932). Fourier transform infrared spectra, FTIR, (Perkin Elmer, USA), ranging from 400 to 4000 cm^{-1} with a resolution of 4 cm^{-1}), were also used to characterize the functional groups of the luffa samples. The surface morphology of the pristine and plasma treated luffa was investigated with a field emission scanning electron microscope SEM (Hitachi 4800) and thermogravimetric

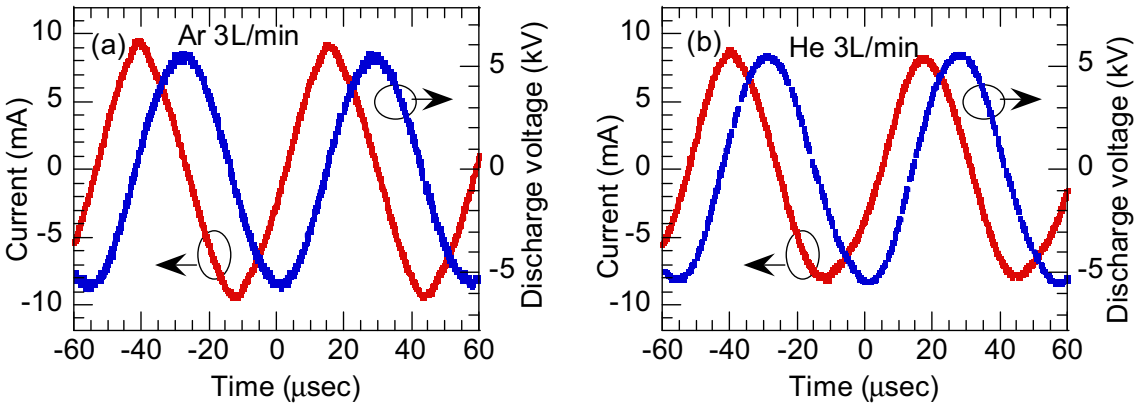

Fig. 2. Voltage-current waveforms of the plasma jet in (a) Ar and (b) He gas.

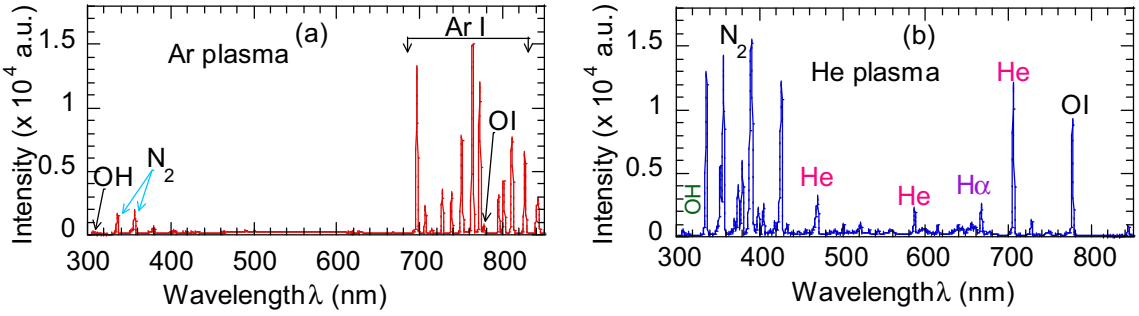

Fig. 3. Optical emission spectra of APPJ in (a) Ar and (b) He plasma.

analysis via Netzsch proteus 70. The temperature range used was from 26 to 1000 °C, at a heating rate of 10 °C min^{-1} under a nitrogen environment. For contact angle, 10 μL of deionized (DI) water or blue ink were dropped on the top of luffa fibers samples and the contact angle was measured by digital microscope.

2 Results and discussion

2.1 Electrical and optical characterization of the APPJ

A typical example of a voltage, $V(t)$, to current, $I(t)$, waveforms of the atmospheric pressure plasma jet in Ar and He discharges is shown in Figure 2, at gas flow rate of 3 l min^{-1}. As clearly seen, the $V(t)$–$I(t)$ waveforms are smooth and fairly sinusoidal. The current waveform does not superimposed with small spikes, implying that the discharges are homogeneous and free from filamentary. The current leads the voltage irrespective of discharge gas type, indicating the capacitive nature of the discharge impedance. The discharge power, P, can be expressed as $P = V_{\rm rms} \times I_{\rm rms} \times \cos(\theta)$, where $V_{\rm rms}$ and $I_{\rm rms}$ are the rms values of the discharge voltage and total current and θ is phase difference, respectively. The computed average discharge power were 7.2 W and 7.5 W for Ar and He discharges, respectively.

The in-situ diagnostics of the active species existing in the Ar and He plasmas give interesting information for understanding the physical/chemical process involved in the plasma treatment of luffa fibers. Figures 3a and 3b show a typical Ar and He plasma emission spectra at a fixed gas flow rate of 3 l min^{-1} and discharge voltage of ~10 kV$_{\rm pp}$. As clearly seen, the Ar plasma spectrum is dominated with Ar I atomic lines such as 696.4 nm, 706.7 nm, 738 nm, 750.2 nm, 763.2 nm, 772.4 nm, 801 nm, 810.6 nm and 841.4 nm. The Ar spectrum is rich in molecular vibrational bands, for instance hydroxyl, OH, (306–309 nm) band. Few peaks belong to nitrogen in the 310–440 nm range, and O I at 777.1 nm, respectively. For He plasma spectrum shown in Figure 3b, it is dominated by neutral He I atomic lines; 388.8 nm, 438.8 nm, 501.6 nm, 587.6 nm, 667.8 nm, 706.5 nm and 728.1 nm. Also, one can observe strong nitrogen molecular bands appearing in the range 310–440 nm, atomic hydrogen H_α at 656.3 nm, atomic oxygen O I at 777.41 nm and at 844.6 nm in He plasma spectrum shown in Figure 3b. The presence of OH, N_2, H_α and O I spectra are ascribed to the dissociation of trace amount of water molecule existing in surrounding air. These species are characterized with long-lived metastable [14] and thus are important as reservoirs of energy promoting plasma surface modification of luffa surface.

2.2 Luffa surface characterization

2.2.1 SEM analysis

The morphology of pristine and plasma treated luffa fiber are shown in Figure 4. SEM images of pristine and plasma

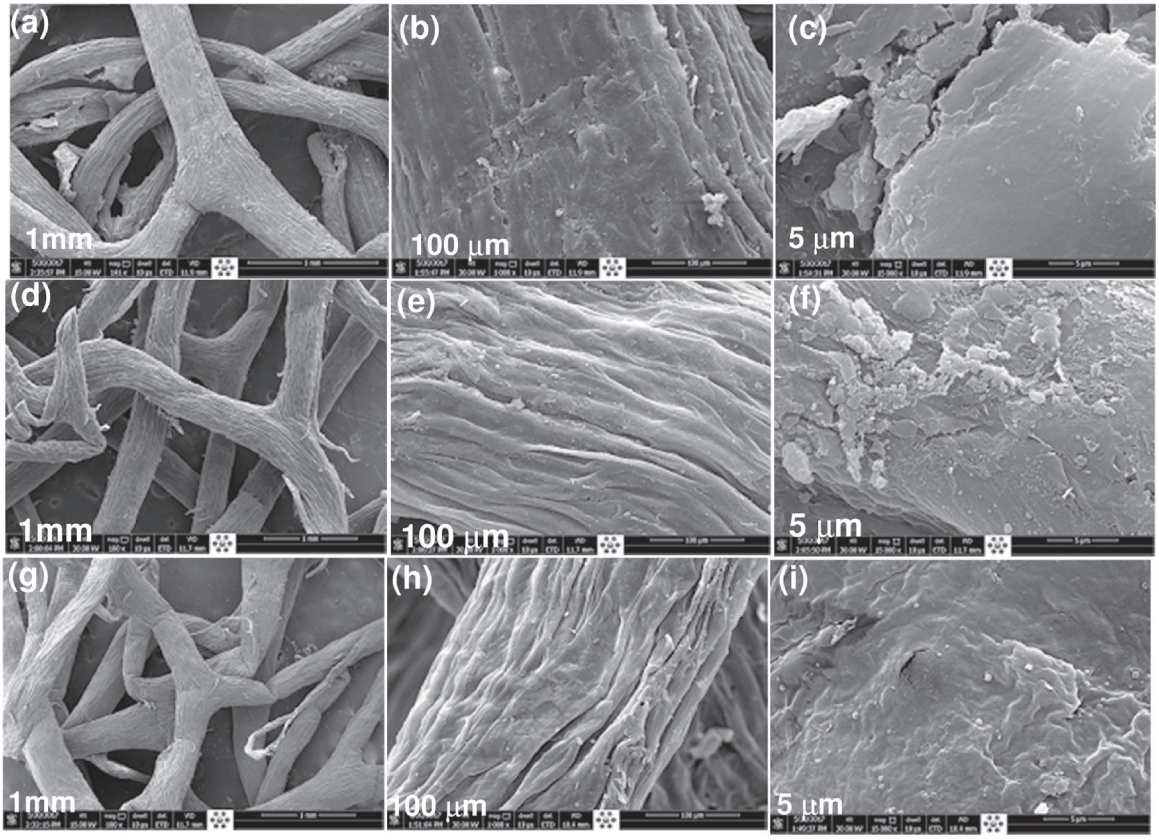

Fig. 4. SEM images of luffa fibers (a,b,c) pristine luffa, (d,e,f) Ar plasma treated luffa and (g,h,i) He plasma treated luffa.

treated luffa fibers have been taken at scales 1 mm, 100 μm and 5 μm, respectively. At scale of 1 mm, the pristine luffa fibers resemble the branch of a tree and preserve the same shape after plasma treatment as can be seen in Figures 4a, 4d and 4g. SEM micrographs (100 μm) of pristine fiber surface show a homogeneous aspect, with an outer lignin rich layer around the fibers. After He or Ar plasma treatment, the luffa fiber surface becomes more wrinkled and roughness increased with small empty channels and lamellar structures as seen in Figures 4e and 4h. This implies that the plasma species remove the hemicellulose and/or lignin outer layers. Thus plasma treatment improve luffa interfacial characters, in particular when luffa fibers are used as filler in polymeric composites, filters and/or as absorption materials. High resolution SEM image confirm the presence of homogeneous-thick lignin layer covering the pristine fiber surface as seen in Figure 4c. After He or Ar plasma treatment, Figures 4f and 4i, tiny bumps and erosion of the fiber inner cellulose framework surface can be observed, indicating grafting of functional groups into the fiber surface. It should be noted that the energetic electrons excited plasma species with the surrounding air, so that some incorporation of O and N from the air is to be expected.

2.2.2 FTIR analysis

The FTIR analysis has been used to explore the luffa fiber's surface composition before and after plasma treatment. FTIR spectra of pristine luffa fiber and plasma treated ones are shown in Figure 5. The FTIR spectra of the pristine luffa shown in Figure 5a reveals prominent absorption peaks at 1026, 2890–2931, 3336.7 cm^{-1} that are common to ligno-cellulosic materials. The absorption peak at 1026 cm^{-1} is assigned to C−C stretching vibrations or COH bending in hemicelluloses [15]. The bands in the range 2890–2931 cm^{-1} and at 3335 cm^{-1} corresponding to the C–H stretching vibrations and OH group present on COH bending in lignin and hemicelluloses, respectively [15]. There are also weak peak at 1730 cm^{-1} that corresponds to C=O stretching vibration of the carbonyl in the xylan component of hemicellulose and lignin [16] and weak bands between 1200 and 1600 cm^{-1} ascribed to aromatic region related to the lignin [17]. The FTIR of He and/or Ar plasma treated luffa fibers shown in Figures 4b and 4c reveals same prominent absorption peaks of the pristine luffa, however, with relative intensities. For instance, peak at 1026 cm^{-1} remarkably decreases in particular for Ar plasma treated luffa sample, probably due to partial elimination of lignin by plasma treatment as confirmed by SEM images (Figs. 4e and 4h). In contrast, bands at 1260 cm^{-1} (C–O bond), 1317 cm^{-1} (OH group), 1450 cm^{-1} (O–C=O bond), 1636 cm^{-1} (O–C=O bond) and 1730 cm^{-1} (C=O bond) slightly increases after plasma treatment. The increase of these oxygen-containing functional groups exited in the plasma-treated luffa fiber provide relatively active sites for next luffa fibers processing step. The band at 3335 cm^{-1} for He plasma treated luffa is much more

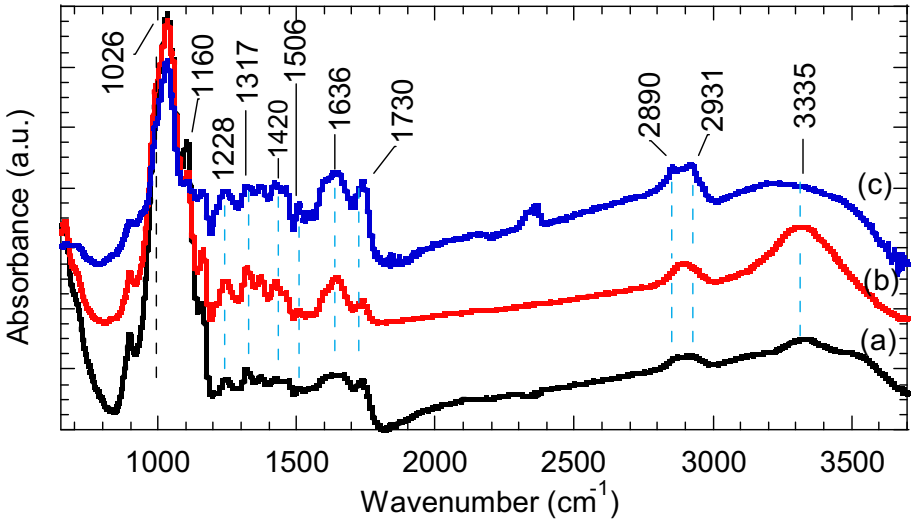

Fig. 5. FTIR spectra of (a) pristine luffa, and after plasma treatment for 40 s, (b) He plasma and (c) Ar plasma, respectively.

intense in comparison to the pristine and argon plasma treated luffa, due to oxidation of the side chain hydrogen type such as methoxy OCH_3 and CH groups linkage to aromatic ring of lignin and formation of extra hydroxyl groups on the luffa surface.

2.2.3 XPS analysis

Figure 6A shows the XPS survey spectra of pristine and plasma treated luffa fibers where carbon, calcium, nitrogen and oxygen can be inferred. The quantitative concentration of the luffa fiber chemical composition is seen in Figure 6B. As can be seen, the ratio O/C increases with the plasma treatment basically due to removal of hemicellulose, lignin, and other contamination on the surface. Apart from these, some contamination by Na (497 eV) and Ca (347 eV), probably introduced during sample handling, can be observed. The O/C ratio in the pristine luffa fiber is (0.18) indicating the rich hemicellulose and/or lignin contents of the outer surface of the luffa fibers [18]. After He or Ar plasma treatment, the O/C ratio jumped to 1.088 and 1.095 for He and Ar plasma respectively. The higher O/C ratio in the plasma treated luffa samples pointing to graft oxygen atoms in the luffa fiber surface and hence synthesized oxygen containing functional group on the luffa fiber outer surface.

High resolution C1s spectra of pristine and plasma treated luffa fiber are shown in Figure 7. As can be seen, the C1s spectra of pristine luffa (Fig. 7a) can be deconvolved into 4 regions, namely 284.4 eV (C=C or CH), 285.5 eV (C–C), 286.6 (CO and/or C–OH) and 289.1 (O=C–HO carboxyl) which agree will with C1s spectra of lignocellulosic materials [18]. The C1s spectra shape of the plasma treated fiber (Figs. 6b and 6c) are remarkably extended for binding energy $\geq$287 eV, which inferred the large component of oxygen containing functionalized group exist in the plasma-treated fiber surface. As can be seen, the C1s of the He or Ar plasma treated fiber can be resolved into 5 peaks; beside the C=C or C–H, C–C and C–O or C–OH groups, there are additional peaks at 288.44 eV and at 290.4 which assigned to O–C–O or C=O carbonyl and O=C–O groups, respectively. In addition, one can noticed the C–C, C=C and O=C–HO bonds remarkably decreases in the plasma treated fiber in comparison with that in the untreated luffa fiber. The XPS results agreed well with FTIR measurements and confirm the efficiency of atmospheric pressure plasma treatment of removing and/or functionalize lignin outer layer of luffa fiber surface. Based on the XPS and FTIR results, the improved surface characteristics of luffa fibers treated in Ar plasma is attributed to Ar ion degrading the lignin by breaking the C–C and/or C–O–C linkage bonds (chain session) forming C=O, O–C=O and C–O bonds upon treated sample exposed to air. Meanwhile, for the luffa treated in helium plasma the enhancement of C=O and OH groups may results in oxidizing the lignin monomer ring and hydrogen type bonding in lignin, respectively.

2.3 Thermogravimetric analysis

Figure 8 shows the thermogravimetric analysis and its first derivatives (DTG) of the pristine and Ar plasma treated luffa fibers. As can be seen in Figure 7a, the TGA graph shows different regions that relates to the mass loss ratio of the sample. For example, the pristine fiber mass decreased –5.17 wt% as temperature increased from 29 to 200 °C, and considerably decreased –68.69 wt% as temperature increased from 201 up to 380 °C. When temperature increased beyond 381 up to 630 °C, it results in reduced mass loss about –26.14%. Similar TGA results of the pristine luffa fiber is reported by Boynard et al. [19]. The TGA trace of the Ar plasma treated luffa fibers mimics that of the pristine one, however, with different mass loss ratio. The mass loss ratio of the Ar plasma treated luffa fibers are –2.78%, –66.34 wt%, –23.63 wt% for temperature increments of 30–200 °C, 201–380 °C and 381–800 °C, respectively. The maximum degradation temperature are 356.4 °C and 361 °C of pristine and Ar plasma treated-luffa, respectively, as seen in Figure 8b. In other words, the Ar plasma treated

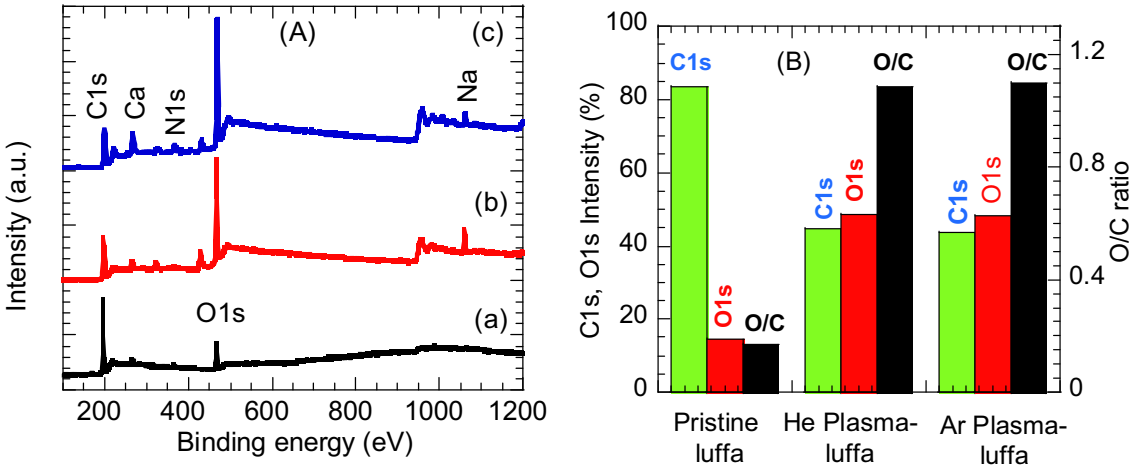

Fig. 6. (A) Survey spectra of luffa (a) pristine, and after plasma treatment for 40 s (b) He plasma and (c) Ar plasma, respectively. (B) Relative intensity of C1s, O1s and O/C ratio for pristine and plasma treated luffa.

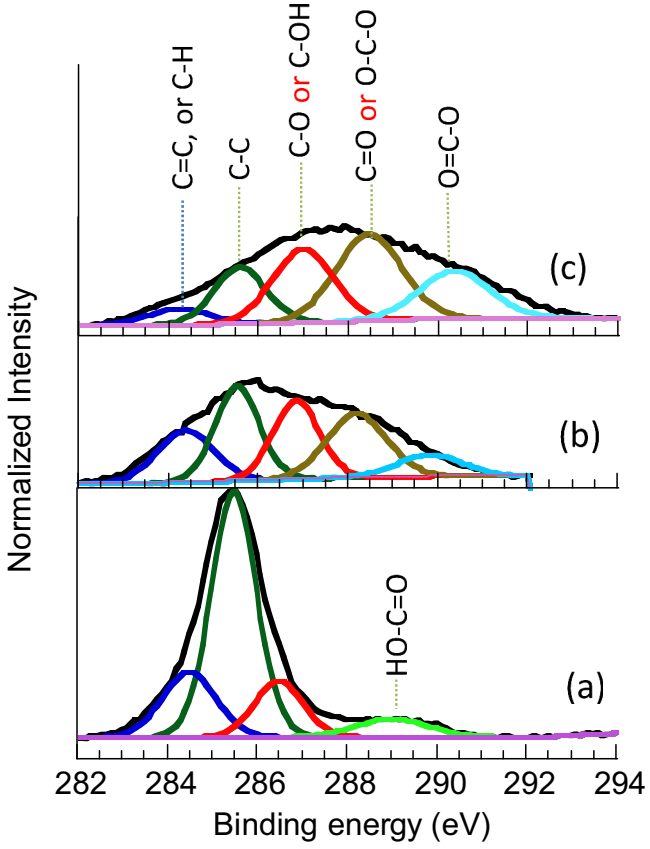

Fig. 7. High resolution C 1s spectra of (a) pristine luffa fibers, (b) luffa treated with He plasma and (c) luffa treated with Ar plasma.

luffa fibers improves thermal stability, in particular at temperature higher than 300 °C. The mass loss as temperature increased up to 200 °C probably attribute to evaporation of the retained water in the samples and removal of lighted molecules. While the mass loss at temperature ≫ 200 °C is due to thermal degradation of hemicellulose (290 °C), cellulose (370 °C) and lignin (280–520 °C) [20,21].

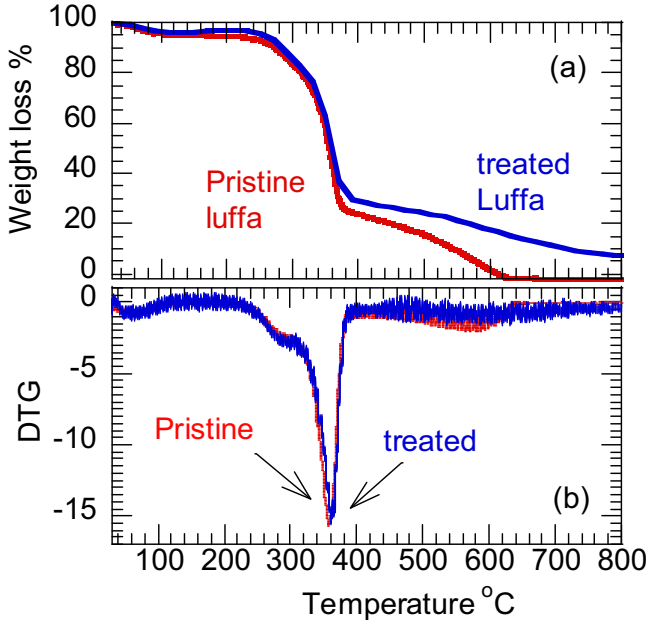

Fig. 8. Thermogravimetric analysis (TGA) of luffa fibers (a) pristine and (b) Ar plasma treated luffa.

At higher temperatures ≫ 600 °C, carbonization occurs with accentuated loss of material, in particular for the Ar plasma treated fiber sample.

2.4 Wettability

Figure 9 shows the different wetting properties of the pristine and plasma treated luffa. As can be seen in Figures 9a and 9b, the water and blue ink droplet deposited on the pristine luffa fibers preserve their spherical shape, with contact angle 120° and 98° for de-ionized water and blue ink, respectively. The high contact angles of the liquid droplets indicate their super-hydrophobic nature of the pristine luffa fibers. Meanwhile, the plasma modified luffa fibers shows super-hydrophilic characters, in which the water as well

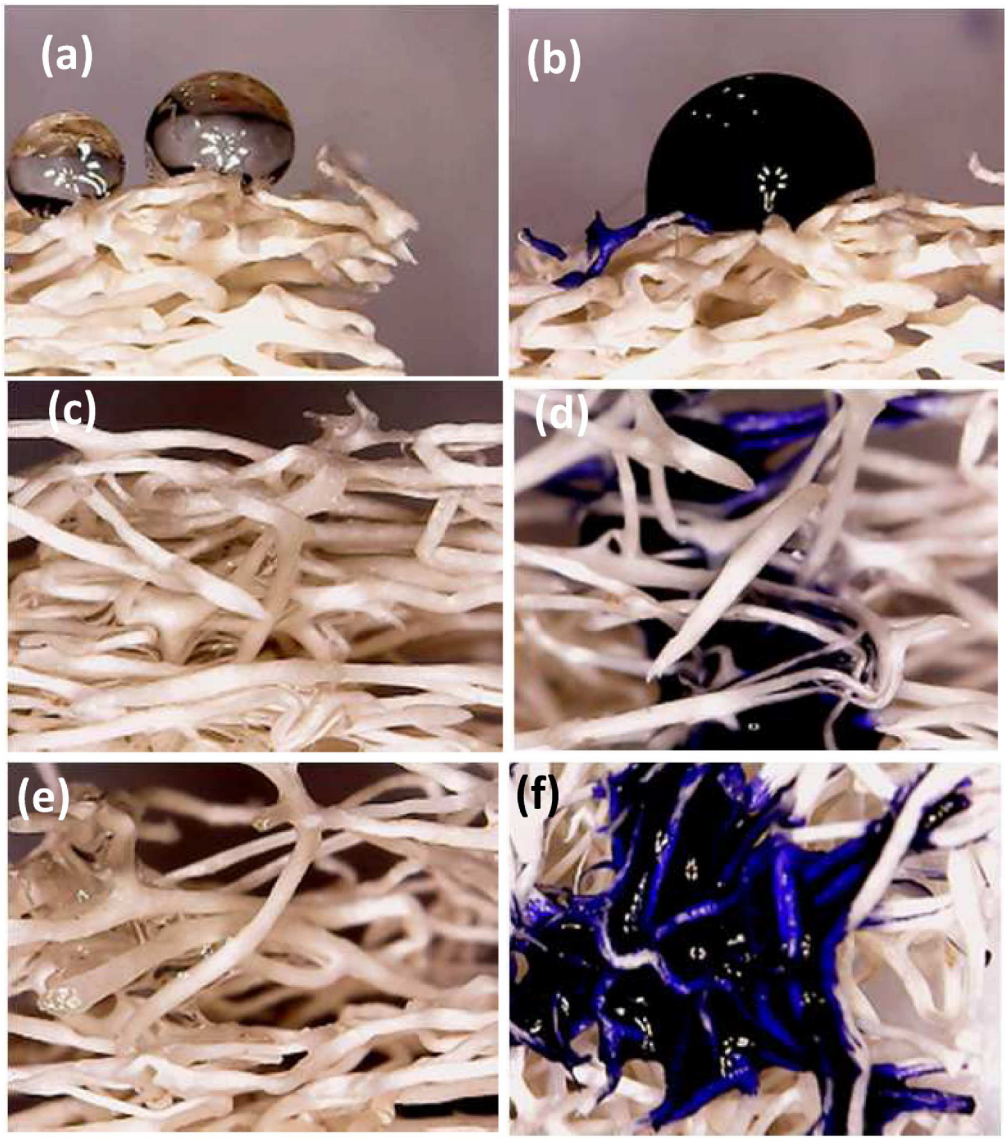

Fig. 9. Contact angle for pristine luffa (a,b) and He plasma treated luffa (c,d) and Ar plasma treated luffa (e,f).

as blue ink spread and absorbed by the fibers as seen in Figures 9c, 9d and Figures 9e, 9f for luffa samples treated with He and Ar plasma, respectively.

3 Summary

The plasma effects on the fibers surface were found to remarkably influence the fiber surface chemical composition and/or surface roughness. As a result, the plasma treatment significantly increased the adhesion character of luffa fibers. This is an advantage of luffa fibers which is used as reinforcement filler of composite materials as well as nano-particles adsorptive medium. Moreover, the plasma treatment preserves the luffa fiber integrity and relatively improves its thermal stability.

The author wishes to thank the reviewers for very careful review of the manuscript, and for corrections and comments that improves the quality of the work.

References

1. J.P. Chen, T.C. Lin, Biotechnol. Progr. **21**, 315 (2005)
2. J. Li, Z. Ren, Y. Ren, L. Zhao, S. Wang, J. Yu, RSC Adv. **4**, 35789 (2014)
3. I.O. Mazali, O.L. Alves, Anais da Academia Brasileira de Cincias **77**, 25 (2005)
4. K.E. Bal, Y. Bal, A. Lallam, Text. Res. J., **73**, 241 (2004)
5. H. Demir, U. Atikler, D. Balkse, F. Tihminlioglu, Compos. Part A: Appl. Sci. Manuf. **37**, 447 (2006)
6. Y. Laidani, S. Hanini, G. Henini, Energy Proc. **6**, 381 (2011)
7. J. Shen, Y.M. Xie, X. Huang, S. Zhou, D. Ruan, J. Mech. Behav. Biomed. Mater. **15**, 141 (2012)
8. J. Shen, Y.M. Xie, X. Huang, S. Zhou, D. Ruan, Int. J. Impact Eng. **57**, 17 (2013)
9. L. Ghali, S. Msahli, M. Zidi, F. Sakli, Mater. Lett. **63**, 61 (2009)

10. S. Goutianos, T. Peijs, B. Nystrom, M. Skrifvars, Appl. Compos. Mater. **13**, 199 (2006)
11. C.A. Boynard, S.N. Monteiro, J.R.M. D'Almeida, J. Appl. Polym. Sci., **87**, 1927 (2003)
12. J. Mejia, J. Fiorelli, H. Savastano, Int. J. Eng. Technol. **7**, 397 (2015)
13. C. Liu, C. Yan, W. Luo, X. Li, W. Ge, S. Zhou, Mater. Lett. **157**, 303 (2015)
14. P. Cullen, V. Milosavljevic, Prog. Theor. Exp. Phys., **6**, 063J01 (2015)
15. V.K. Gupta, S. Agarwal, P. Singh, D. Pathania, Carbohydr. Polym. **98**, 1214 (2013)
16. Y. Kataoka, T. Kondo, Macromolecules **31**, 760 (1998)
17. X. Colom, F. Carrasco, P. Page's, J. Canavate, Compos. Sci. Technol. **63**, 161 (2003)
18. A. Toth, O. Faix, G. Rachor, I. Berto ti, T. Szekely, Appl. Surf. Sci., **72**, 209 (1993)
19. C.A. Boynard, J.R.M. D'Almeida, Technol. Eng. **39**, 489 (2000)
20. B.L. Browning, *The Chemistry of Wood* (Inter science, New York, NY 1963)
21. T. Nguyen, E. Zavarin, E.M. Barrall, J. Macromol. Sci. Part C **21**, 1 (2007)